Kinetics of H^+ Ion Binding by the $P^+Q_A^-$ State of Bacterial Photosynthetic Reaction Centers: Rate Limitation within the Protein

Péter Maróti and Colin A. Wraight
Center for Biophysics and Computational Biology, and Department of Plant Biology, University of Illinois, Urbana, IL 61801-3838 USA

ABSTRACT The kinetics of flash-induced H^+ ion binding by isolated reaction centers (RCs) of *Rhodobacter sphaeroides*, strain R-26, were measured, using pH indicators and conductimetry, in the presence of terbutryn to block electron transfer between the primary and secondary quinones (Q_A and Q_B), and in the absence of exogenous electron donors to the oxidized primary donor, P^+, i.e., the $P^+Q_A^-$ state. Under these conditions, proton binding by RCs is to the protein rather than to any of the cofactors. After light activation to form $P^+Q_A^-$, the kinetics of proton binding were monoexponential at all pH values studied. At neutral pH, the apparent bimolecular rate constant was close to the diffusional limit for proton transfer in aqueous solution ($\sim 10^{11}$ M^{-1} s^{-1}), but increased significantly in the alkaline pH range (e.g., 2×10^{13} M^{-1} s^{-1} at pH 10). The average slope of the pH dependence was −0.4 instead of −1.0, as might be expected for a H^+ diffusion-controlled process. High activation energy (0.54 eV at pH 8.0) and weak viscosity dependence showed that H^+ ion uptake by RCs is not limited by diffusion. The salt dependence of the H^+ ion binding rate and the pK values of the protonatable amino acid residues of the reaction center implicated surface charge influences, and Gouy-Chapman theory provided a workable description of the ionic effects as arising from modulation of the pH at the surface of the RC. Incubation in D_2O caused small increases in the pKs of the protonatable groups and a small, pH (pD)-dependent slowing of the binding rate. The salt, pH, temperature, viscosity, and D_2O dependences of the proton uptake by RCs in the $P^+Q_A^-$ state were accounted for by three considerations: 1) parallel pathways of H^+ delivery to the RC, contributing to the observed (net) H^+ disappearance; 2) rate limitation of the protonation of target groups within the protein by conformational dynamics; and 3) electrostatic influences of charged groups in the protein, via the surface pH.

INTRODUCTION

In the reaction center (RC) complex of purple photosynthetic bacteria, the light-induced charge separation leads to the formation of a metastable state, in which the primary donor (P, a bacteriochlorophyll dimer) is oxidized, and tightly bound quinone (Q_A) is reduced to the semiquinone state. The electron can then be transferred to a second, reversibly bound quinone (Q_B), which acts as a two-electron gate (Wraight, 1982). Protonation state changes are also associated with the electron transfer events, especially in the reduction of the quinones. If P^+ is rereduced by a secondary donor (*c*-type cytochrome in vivo), a second flash-induced turnover of the RC results in the double reduction of Q_B to quinol with the net uptake of two H^+ (for reviews, see Okamura and Feher, 1992, 1995; Shinkarev and Wraight, 1993; Sebban et al., 1995).

In isolated RCs from *Rhodobacter sphaeroides*, there is no endogenous secondary electron donor to rereduce P^+, and unless an exogenous donor is added, the charge separation state recombines after each flash in 0.1–1 s, depending on the functionality of Q_B. The one-electron states of the quinones (Q_A^- and Q_B^-) are accompanied by H^+ binding, but the protonation targets are residues of the protein rather than the semiquinones themselves (Wraight, 1979). Flash-induced proton binding by the RC, after a single flash, arises from pK shifts to higher values for various protonatable groups, under the electrostatic influence of the anionic semiquinones. Extensive measurements of the proton binding stoichiometry showed that a minimum of four or five separate acid-base groups are involved in the proton uptake after a flash, with pK shifts of 0.5–1.5 pH units (Maróti and Wraight, 1988a,b; McPherson et al., 1988; Shinkarev et al., 1989; Maróti et al., 1995), and possibly many more with correspondingly smaller pK shifts (McPherson et al., 1988). The stoichiometry of protons bound per RC depends on the protonation and redox states of the primary donor, P, as well as of Q_A and Q_B (Maróti and Wraight, 1988a,b; McPherson et al., 1988). Thus if no donor is present for P^+ reduction, significant amounts of H^+ binding (>0.1 H^+/RC) by RCs are observed only in the alkaline pH range ($7 < pH < 11$). The pK values and shifts depend on which quinone is charged and whether the Q_B pocket is occupied.

A kinetic correlation also exists between H^+ binding and electron transfer to Q_B. Both first and second electron transfer rates in the quinone complex are pH dependent, especially above pH 8–9, and electron and proton transfer events are coupled (Wraight, 1979; Kleinfeld et al., 1984, 1985; Maróti and Wraight, 1989a, 1990; Graige et al., 1996). For the first electron transfer, bound protons in the vicinity of the Q_B binding site are involved in stabilizing the semiquinone. For the second electron transfer, protons must

Received for publication 23 January 1997 and in final form 4 April 1997.

Address reprint requests to Dr. Colin A. Wraight, Department of Plant Biology, 190 ERML/MC-051, University of Illinois, 1201 West Gregory Drive, Urbana, IL 61801-3838. Tel.: 217-333-3245; Fax: 217-244-1336; E-mail: cwraight@uiuc.edu.

Dr. Maróti's permanent address is Institute of Biophysics, József Attila University, Egyetem utca 2, Szeged, H-6722, Hungary.

0006-3495/97/07/367/15 $2.00

be delivered to the quinone headgroup itself in the reduction to quinol (Takahashi and Wraight, 1990; Paddock et al., 1990).

It has recently been established that the second electron transfer is "activated" by the transient protonation of Q_B^-, forming Q_BH, and that H^+ uptake is not rate limiting (Graige et al., 1996). Indeed, if electron transfer to Q_B were rate-limited by proton transfer, the implied rate constants for proton transfer, at high pH, would be improbably large. However, the kinetics of H^+ binding have been measured directly and yield apparent bimolecular rate constants that are anomalously large ($>10^{12}$ M^{-1} s^{-1}; Maróti and Wraight, 1989b; Takahashi et al., 1992). When electron transfer to Q_B is blocked by an inhibitor, which competitively displaces the secondary quinone, similarly large proton binding rates at high pH are evident, both in measurements by indicator dyes (Maróti and Wraight, 1989b) and in the electric potential generation associated with charge movements in the quinone region (Drachev et al., 1990). Under these conditions, the observed H^+ binding is a direct response to the almost instantaneous formation of $P^+Q_A^-$. We describe here the kinetic aspects of light-induced H^+ binding in terbutryn-blocked RCs. The experimental results on the effects of pH, salt concentration, temperature, viscosity, and deuteration on the rate of H^+ (or D^+) binding to the RC in the $P^+Q_A^-$ state will be discussed in terms of mechanisms of proton delivery to, and accessibility of, the protonatable groups in the protein.

MATERIALS AND METHODS

Reaction centers from *Rb. sphaeroides,* strain R-26, were isolated as detailed earlier (Maróti and Wraight, 1988a). The RC stock (usually ~100 μM) was dialyzed against 1 mM Tris buffer (pH 8.0), 0.03% Triton X-100 before use. RCs isolated this way showed little secondary quinone activity. However, terbutryn, a potent inhibitor of electron transfer between Q_A and Q_B, was routinely present at a concentration of 60 μM (Stein et al., 1984). The concentration of terbutryn used was much higher than the I_{50} for Q_B inhibition (<5 μM, even in the presence of added quinone; Stein et al., 1984). The concentration of RCs was determined by the light-induced absorbance change due to P^+ at 430 nm, using an extinction coefficient of 26 mM^{-1} cm^{-1}.

After dilution of the RC stock in the experimental sample, which was routinely degassed by bubbling nitrogen gas and included 0.03% Triton X-100, the Tris buffer content was ~10 μM, which constituted a negligible buffering capacity, even at pH 8.0. Conductance measurements of various samples, after pH adjustment and inclusion of pH indicator dye (40 μM), gave values of ~3×10^{-5} S, equivalent to 100 μM KCl, before the addition of any exogenous salts.

H^+ binding by reaction centers was detected by two independent methods: optically, using pH indicator dyes, and electrically, by a conductimetric assay. A comprehensive analysis and comparison of the two methods has been presented (Maróti and Wraight, 1988a):

1. The flash-induced absorbance change of the pH indicator dye was monitored at the isosbestic wavelength of the $PQ_A \rightarrow P^+Q_A^-$ transition (near 586 nm) using a locally constructed kinetic spectrophotometer. The true H^+ binding was obtained by subtracting the signal of a buffered sample to eliminate the contribution of any electrochromic responses of bound dyes. The time resolution of ~30 μs was limited by the finite duration of the exciting xenon flash (EG&G FX-200) and by the recovery time of the electronics (photomultiplier + amplifier) after the flash artifact. The time constant was routinely set low to minimize the recovery time. Between 32 and 256 traces were averaged. The indicators used were (in order of increasing pK): bromcresol purple, phenol red, bromthymol blue, cresol red, *m*-cresol purple, *o*-cresol phthalein, thymol blue, thymol phthalein. These are all of the anionic variety: $HIn^- \leftrightarrow In^{2-} + H^+$.

2. The electrical conductance changes related to H^+ ion binding by the RCs were evaluated by the buffer-pair method (Maróti and Wraight, 1988a): a zwitterionic buffer gains charge and a cationic buffer loses charge upon deprotonation. Subtraction of the conductance changes measured in the two types of buffers yields the net H^+ binding signal, as coherent effects like heat and non-proton-related ion changes cancel out. The kinetics from each buffer sample were averaged over 50–250 traces. The locally designed conductimeter (described in Maróti and Wraight, 1988a) was slightly modified for fast kinetic measurements: a low internal time constant (100 μs) and a high frequency (106 kHz) were selected for the lock-in amplifier (Princeton Applied Research, model 120), and the measuring cell was shielded from the high-frequency electrical noise of the flash discharge by a grounded copper box (Faraday cage). Buffer pairs used in this work were 10 mM bis-Tris-propane and 10 mM CHES at pH 9.5; 10 mM aminomethylpropanol and 10 mM glycine at pH 10.0; 20 mM methylamine, 5 mM piperidine, and 40 mM CAPS at pH 10.8; and 25 mM piperidine and 20 mM CAPS at pH 11.1. The electric conductances of the cells with cationic and zwitterionic buffers were equalized by adding salt to less than 5 mM final concentration.

For deuterium substitution and D^+ binding measurements, the RCs from a highly concentrated stock (>300 μM) were diluted into D_2O (generously provided by Dr. J. R. Norris, Argonne National Laboratory) containing, typically, 100 mM KCl, 60 μM terbutryn, and 0.03% Triton X-100. The H_2O content of the sample was less than 1%. The pD of the solution was measured by a glass electrode that had been standardized with conventional buffer mixtures (in H_2O) at pH 7.0 and 11.0, according to the expression

$$pD = \text{apparent pH} + 0.40$$

where "apparent pH" means the actual pH meter reading (Mikkelson and Nielson, 1960; Glasoe and Long, 1960). Deuterated acid (DCl) and base (NaOD) (both from Sigma Chemical Co., St. Louis) were used for pD adjustment. The indicator dyes for stoichiometric measurements were calibrated by mixing DCl standards and D_2O (for dilution correction) in the sample.

The pK values for several indicators were determined by optical assay of direct acid-base titrations, using lower concentrations of indicators (2–10 μM) than in the kinetic measurements of flash-induced proton binding, to enhance the RC-to-dye ratio. The net binding of indicator by RCs was investigated for thymol blue by equilibrium chromatography. A 1 × 30 cm column of Sephadex G-75 was preequilibrated with indicator at a set pH and salt concentration. RCs, previously dialyzed against an identical buffer, including indicator, were loaded onto the column and eluted with the same buffer. Fractions collected were assayed spectrophotometrically for RC and indicator concentrations. Indicator was assayed in the colored alkaline form after adjusting the pH to well above the pK.

RESULTS

The pH dependence of the apparent rate of proton binding

The kinetic events after a single, short actinic flash are greatly simplified if the electron transfer from Q_A^- to Q_B is blocked by extracting the secondary quinone and/or adding terbutryn to inhibit Q_B function. The time course of the pH indicator response to H^+ uptake by the $P^+Q_A^-$ state of the RC was fit well by a single exponential (Fig. 1 *B*), with an apparent rate constant of 10^4–10^3 s^{-1}, in the pH range 7–10. A biexponential analysis occasionally yielded a second component of small and irregular amplitude, without sig-

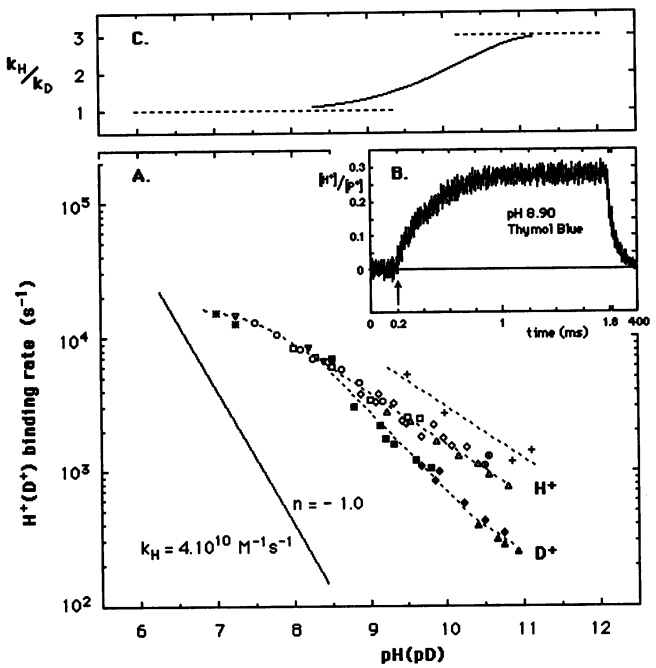

FIGURE 1 Kinetics of H^+ (D^+) binding by isolated RCs. (*A*) pH (pD) dependence of observed H^+ (D^+) binding rates and comparison of spectrophotometric and conductimetric measurements. Conditions for spectrophotometric assay: H^+ binding-100 mM NaCl, 0.03% Triton X-100, 60 μM terbutryn, 1.3 μM RC; D^+ binding (in ≥98% D_2O)-100 mM KCl, 0.03% Triton X-100, 60 μM terbutryn, 2.2 μM RC, 23°C. All samples plus 20–40 μM pH (pD) indicator dye as follows: (*open symbols*, H^+; *closed symbols*, D^+) bromocresol purple (*), phenol red (▽, ▼), cresol red (○, ●), *m*-cresol purple (□, ■), thymol blue (◇, ◆), *o*-cresol phthalein (△, ▲), and thymol phthalein (⊙). Conditions for conductimetric assay (+): 0.03% Triton X-100, 60 μM terbutryn, 2.5 μM RC, 23°C, plus buffer pairs as described in Materials and Methods. The solid line indicates the expected behavior for a diffusion-controlled protonation reaction, with bimolecular rate constant $k_H = 4 \times 10^{10}\ M^{-1}\ s^{-1}$. (*B, inset*) Kinetics of net H^+ binding (unbuffered-minus-buffered signal), at pH 8.90, with thymol blue as indicator; average of 96 traces. Note the change in time scale at 1.8 ms. (*C*) Kinetic isotope effect on the rate of H^+ (D^+) binding, derived from *A*.

nificantly affecting the parameters of the major component. The kinetics of the H^+ rerelease follow those of the charge recombination: $P^+Q_A^- \rightarrow PQ_A$, with a characteristic rate constant of $\sim 10\ s^{-1}$. As the rates of response to H^+ uptake and rerelease differ by at least 100-fold under all conditions studied here, their temporal separation was straightforward and the parameters of proton binding were obtained by single-component exponential fitting of the kinetic traces.

Fig. 1 *A* shows the rate of H^+ uptake (net binding) between pH 7 and 11, using two independent methods: spectroscopy (pH indicator dyes) and electric conductimetry. Beyond these pH values, the amount of H^+ bound to the $P^+Q_A^-$ state becomes too small for reliable kinetic analysis (Fig. 3, and Maróti and Wraight, 1988a). The observed proton binding rates measured with different dyes, as well as the rates measured with a single dye at different pH values, exhibit a continuous dependence. The rates obtained by the conductimetric method are shifted slightly toward higher values, because of the low salt conditions required for these measurements (see Fig. 2 for the salt dependence of the proton binding rate). Taking this into account, the coincidence of the two sets of data is clear. This seems to support the notion that the kinetic data are a real reflection of events in the bulk phase. However, the measurements are indirect, reflecting the ultimate deprotonation of indicator or buffer, and this issue will be returned to in the Discussion. For the time being we will refer to the measured response as H^+ binding or uptake. Fig. 1 reveals two potentially anomalous features of the H^+ binding response:

1. The pH dependence of the rate does not correspond to a slope of $n = -1$, but shows a much smaller average slope (−0.4), with some curvature.

2) The value of the bimolecular rate constant, k_H, using the prevailing H^+ ion concentration ($k_H = k^{obs} \times 10^{pH}$), is pH dependent. The calculated value, at pH 7, is $\sim 10^{11}\ M^{-1}\ s^{-1}$, somewhat larger than expected for a diffusion-limited protonation reaction of a protein in solution (Gutman and Nachliel, 1990), but it is much larger at high pH. At pH 10.0, for example, $k_H \approx 10^{13}\ M^{-1}\ s^{-1}$, nearly three orders of magnitude greater than a reasonable solution value.

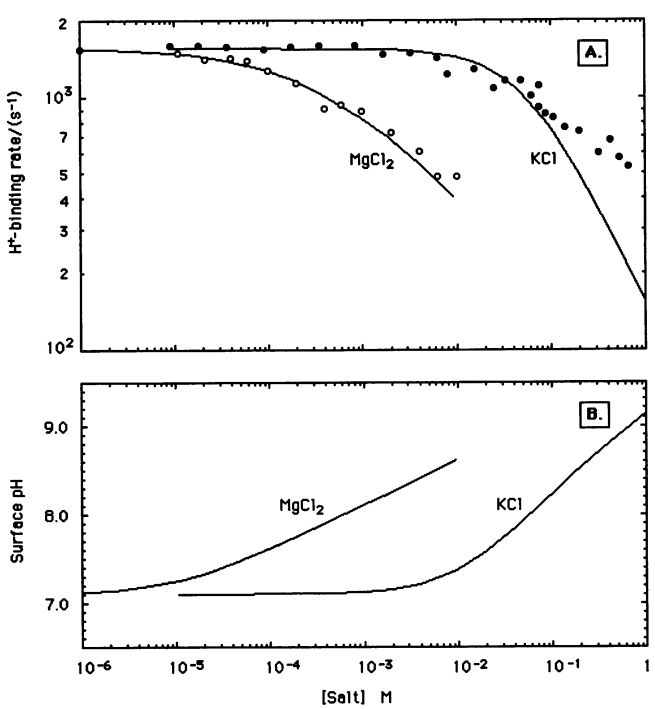

FIGURE 2 Effect of surface potential on the H^+ binding rate. (*A*) Titration of the H^+ binding rate by mono- and divalent cations. Conditions: 3 μM RC, pH 10.0, 0.03% Triton X-100, 60 μM terbutryn, 40 μM *o*-cresol phthalein, monitoring wavelength 586 nm. The rates in $MgCl_2$ (○) and in KCl (●) were fitted with theoretical curves according to Eqs. 10–12, as described in the text, with $\sigma = -0.85\ q/nm^2$, background monovalent cations (c_b') = 100 μM, background divalent cations (c_b'') = 10 μM, proton donor pK = 8.1, $k = 4 \times 10^7\ M^{-1}\ s^{-1}$. (*B*) Expected variation in surface pH during cation titrations of *A*, derived from Eqs. 10–12.

Binding of indicators by isolated reaction centers

An earlier study by Petty and Dutton (1976), utilizing pH indicators to follow proton binding by chromatophore (membrane) preparations from *Rb. sphaeroides*, showed that most dyes used (similar to those in this work) did not bind significantly to the membrane. We checked for such behavior in isolated RCs with a few selected indicators (bromthymol blue, cresol red, thymol blue) and obtained very different results. Net binding of thymol blue by RCs, for example, determined by equilibrium chromatography, showed a linear relationship between RC concentration and dye bound, implying saturated binding. Accumulation of indicator in the fractions containing RCs showed substantial binding at pH 8.5, and less but still significant binding at pH 10.5 (Table 1). At pH 10.5, the net binding of indicator increased slightly at high salt concentrations.

Binding of the indicators to RCs also caused a substantial shift of the dye pK to higher values (Table 2). The magnitude of the pK shift decreased at high salt, largely because of an increase in the control value, without RCs.

In contrast to the effect of RCs, 0.03% Triton X-100 alone (~1 μM micelles; 5–10 dye molecules per micelle) did not affect the pK of any of these dyes, showing that the detergent micelles did not preferentially bind either the protonated (HIn^-) or deprotonated (In^{2-}) states of the indicators. This is in contrast to the observations of Gutman et al. (1981) with bromcresol green, an indicator of general structure similar to ours, and Brij 58, a nonionic detergent with properties and structure similar to those of Triton, but with an alkyl rather than an aromatic hydrophobic moiety. Using very high ratios of detergent to dye (0.1–0.5 dye molecule per micelle), they found that the pK of bromcresol green was shifted to significantly higher values (ΔpK = 1.5), because of preferential adsorption of the protonated species, which has a single negative charge. It is possible that the very low ratios of detergent to dye used in our experiments did not result in significant net adsorption to micelles.

Salt dependence of the H^+ ion binding rate and stoichiometry

The effect of salts on the H^+ uptake kinetics, using both mono- and divalent cations, is shown in Fig. 2 *A*. The rate was constant below a definite threshold salt concentration, but decreased above it. The minimum effective concentration for the divalent cation, Mg^{2+}, was about two orders of magnitude lower than that of the monovalent cation, K^+.

TABLE 1 Binding of thymol blue (TB) to reaction centers

pH*	Conditions#	NaCl	TB/RC
10.5	RCs only	—	2.7 ± 0.1
	RCs + TX	—	1.8 ± 0.2
	RCs + TX	100 mM	2.4 ± 0.1
	RCs + TX	500 mM	5.2 ± 0.6
8.5	RCs + TX	100 mM	15 ± 2

*Buffer was 10 mM CAPS (pH 10.5) or 10 mM glycyl-glycine (pH 8.5).
#"RCs only" indicates no added Triton X-100 (TX), with residual detergent of <0.003% LDAO, <0.001% TX; + TX indicates 0.03% Triton X-100 added.

In 100 mM monovalent salt, the stoichiometries of flash-induced H^+ binding to the $P^+Q_A^-$ state (Fig. 3) were very similar to those reported earlier (Maróti and Wraight, 1988a; McPherson et al., 1988). Flash-induced proton binding by RCs occurs as a result of shifts in the pKs of ionizable groups, induced by the new charge states of the cofactors—P^+, Q_A^-, etc. Over the readily accessible pH range, pH 7–11, the stoichiometries were adequately accounted for by light-induced pK shifts of two components (or groups, see below), although three are required to account additionally for the behavior in the presence of donors (i.e., the PQ_A^- state) in this pH range, and a fourth is needed to extend it to lower pH (Maróti and Wraight, 1988b).

Fig. 3 shows the fits to Eq. 1, with two components (i = 1 and 2), with pK values pK_i^d ("dark," before the flush) and pK_i^l ("light," after the flash):

$$\frac{H^+}{P^+} = \sum_i \left(\frac{10^{pK_i^l - pH}}{1 + 10^{pK_i^l - pH}} - \frac{10^{pK_i^d - pH}}{1 + 10^{pK_i^d - pH}} \right) \quad (1)$$

Interpretation of the magnitude of the pK shifts is model dependent, depending on how many functional groups are invoked to account for the observed H^+ stoichiometry. Assumption of a single group for each component, i, in Eq. 1 yields the largest shifts. Thus the largest reasonable value associated with $P^+Q_A^-$ is a shift of ~1 pH unit for a single group (group 1 in Table 3) with a dark pK ≈ 9.6 in 100 mM KCl (Maróti and Wraight, 1988a). Group 2 has a lower dark-adapted pK ≈ 8.0 and undergoes a smaller pK shift. An alternative interpretation would assign many groups to each component, all undergoing much smaller shifts (McPherson et al., 1988). Collectively, however, they are characterized by the same "apparent" pK values shown.

Fits based on Eq. 1 (Figs. 3 and 7, below) are very sensitive to the choice of pK values, and these are consequently determined to ±0.05 or better. The effects of salts on the ionization properties of the two groups are summarized in Table 3. Divalent cations lowered the pK values of the high pH protonatable group much more than did monovalent cations, at equivalent ionic strength. The pK of the second putative protonatable group around pH 8 was also slightly modified. The maximum amount of protons bound per RC (the peak in the stoichiometry curve) was not much changed under different salt conditions. However, the integrated area under the curves, a reflection of the net free energy change associated with H^+ binding (McPherson et al., 1988), was diminished in divalent cation solutions.

Additional experiments demonstrated that cations induce shifts in apparent pK values for all forms of the quinone complex: Q_A^- in terbutryn-inhibited RCs (this work) or in Q_B-extracted RCs (not shown), and Q_B^- in quinone-supplemented RCs (Shinkarev et al., 1992). In all cases, the influence of divalent cations is much greater than that of

TABLE 2 Effects of Triton X-100 and reaction centers on the apparent pK values of various pH indicators

Indicator	NaCl	pK			ΔpK (±RCs)
		Control*	+ TX#	+RCs	
Thymol blue§	10 mM	8.9	8.95	10.15	1.25
	100 mM	9.3	—	10.3	1.0
	500 mM	9.35	—	10.2	0.85
Cresol red¶	100 mM	8.15	8.15	8.9	0.75
Bromthymol blue‖	10 mM	8.2	—	8.6	0.4
	100 mM	—	—	8.6	

*Indicator in aqueous solution (no detergent or RCs).
#0.03% Triton X-100.
§5–10 μM thymol blue and 4 μM RCs/0.03% Triton X-100, when present.
¶6–10 μM cresol red and 4 μM RCs/0.03% Triton X-100, when present.
‖5 μM bromthymol blue and 1.4 μM RCs/0.03% Triton X-100, when present.

monovalent cations, even at equal ionic strength, indicating that the effect is via alterations in the surface potential and the quantity of mobile charge in the diffuse double layer (Barber, 1980).

Temperature dependence of the proton binding rate

The temperature dependence of the proton binding rate was measured in aqueous solution between 310 and 274 K at different pH values (Fig. 4). With decreasing temperature, the rates declined steadily and were reasonably well fit by linear Arrhenius plots. The apparent activation energies/enthalpies (E_a), calculated from the slopes, were large and were the same in D_2O and H_2O, within the error of the measurement (E_a = 0.41 ± 0.02 eV at pD 10.0, not shown). At pH 8, with cresol red as the indicator, the energy of activation was greater than at pH 10, using *o*-cresol phthalein. Comparison of pH 9 (E_a = 0.45 ± 0.04 eV) and pH 10.2 (E_a = 0.42 ± 0.03 eV, not shown), using thymol blue for both, showed an insignificant change.

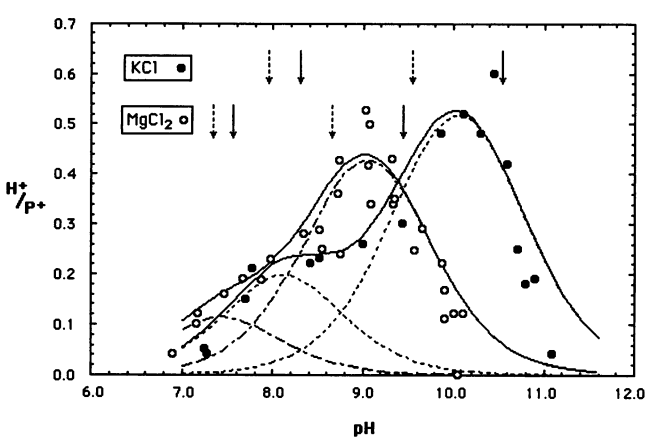

FIGURE 3 Effect of cations on the stoichiometry of proton binding (H^+/P^+) versus pH. Conditions: 1 μM RC, 0.03% Triton X-100, 20 μM Q-10, 60 μM terbutryn, 40 μM pH indicator dye depending on the pH, as in Fig. 1. The ionic strength (100 mM) was set with either monovalent cations (100 mM KCl, ●), or divalent cations (33 mM $MgCl_2$, ○). The curves are drawn assuming two noninteracting protonatable groups with dark (PQ_A, ⇢) pK values of 9.55 and 7.95 (KCl), or 8.65 and 7.35 ($MgCl_2$), and light ($P^+Q_A^-$, →) pK values of 10.55 and 8.3 (KCl), or 9.45 and 7.55 ($MgCl_2$).

H^+ ion binding rate versus viscosity

In contrast to the pronounced temperature sensitivity of the proton binding kinetics, the rate at pH 10.0 was only slightly modified by the viscosity of the solution (Fig. 5). The weak viscosity dependence of the proton binding rate was confirmed at 293 K both with pH indicator dyes and by the conductimetric method. At relatively low viscosities, the two sets of data ran roughly parallel, with slopes of about −0.15. However, at higher values (>8 × 10^{-3} Pa s (centipoise) in H_2O), the measurement failed drastically, and no kinetics were detectable. Because the dependence of the rate at low viscosity was slight, the activation energies calculated from Arrhenius plots in the temperature range 274–312 K (Fig. 4) were not corrected for changes in viscosity.

Kinetics and stoichiometry of D^+ binding in D_2O

The pD dependence of the D^+ binding rate for RCs in D_2O showed anomalous properties similar to those of H^+ binding: deviation from a slope of −1 and apparent enhancement of the bimolecular rate constant, at high pD, compared to values for chemical reactions in solution (Fig. 1 *A*). Close to neutral pH (pD), the H^+ and D^+ binding rates did not differ within the experimental error, but at increasing pH (pD) the binding rates diverged, with D^+ binding being slower. Above pH (pD) 10.0, the D^+ binding rate (k_D) appeared to tend toward a steady relative value of about one-third of the proton binding rate (Fig. 1 *C*), i.e., an isotope effect, k_H/k_D, of 3.

The rate of D^+ binding by RCs was measured as a function of incubation time in D_2O, at a fixed pD value of 10.2. This is shown in Fig. 6 as the isotope effect, k_H/k_D, where k_H is the rate in H_2O at pH 10.2. After dilution into D_2O, the isotope effect is initially large but subsequently declines, i.e., a normal, prompt isotope effect ($k_H/k_D > 1$) followed by a slow inverse effect. Measurements carried out

TABLE 3 Effect of cations and D_2O on the dark and light pK values of the two high pK proton-binding groups.

	Group 1			Group 2		
	Dark pK	Light pK	$\Delta pK^{(l-d)}$	Dark pK	Light pK	$\Delta pK^{(l-d)}$
Monovalent cation						
10 mM KCl	10.0	10.8	0.8	8.9	9.5	0.6
100 mM KCl	9.55	10.55	1.0	7.95	8.3	0.35
Divalent cation						
33 mM $MgCl_2$	8.65	9.45	0.8	7.35	7.55	0.2
Deuteration						
100 mM KCl	9.85	10.85	1.0	8.25	8.4	0.15
ΔpK (D − H)	0.3	0.3		0.3	0.1	

Values in this table are derived from the data of Figs. 3 and 7, analyzed by Eq. 1. See text for definition of the term "group."

with different pH indicator dyes gave similar results, indicating that both the prompt and the slow effects reflect changes upon deuteration in the protein rather than the indicator dye. In the experiment shown, the rate initially decreased by 40%, and the half-time of the subsequent partial recovery was ~6 h. The changes in the apparent binding rate were reversible: upon dilution in H_2O and ultrafiltration of the RCs, the rate was restored to a value typically measured in H_2O.

Analysis of the D^+ binding stoichiometry with Eq. 1 revealed shifts of +0.1 to +0.3 units in the pKs of the groups involved (Fig. 7 and Table 3). The isotope shift occurs "promptly" (i.e., within 2 h, the time needed to measure the stoichiometry over a range of pD), and no further changes in the stoichiometry were observed after prolonged (24 h) incubation in D_2O. D_2O induced somewhat larger shifts in pK values in titrations of a pH indicator dye (*m*-cresol purple: $\Delta pK = pK_D - pK_H = +0.60$) and a protonatable amino acid [L-cysteine: $\Delta pK_2 = +0.4$ ($-SH/-S^-$) and $\Delta pK_3 = +0.8$ ($-NH_3^+/-NH_2$)] (data not shown).

DISCUSSION

This work has revealed that the measured response to flash-induced H^+ ion binding, by RCs in the $P^+Q_A^-$ state, has kinetic features that appear to deviate strongly from those expected of a simple bimolecular collisional (encounter) process limited by H^+ ion diffusion in the bulk phase. In particular, the pseudo-first-order rate constant is only weakly pH dependent, leading to a calculated bimolecular rate constant that is pH dependent and attains very large values in the alkaline pH range. Furthermore, the temperature dependence is steep, whereas the viscosity dependence

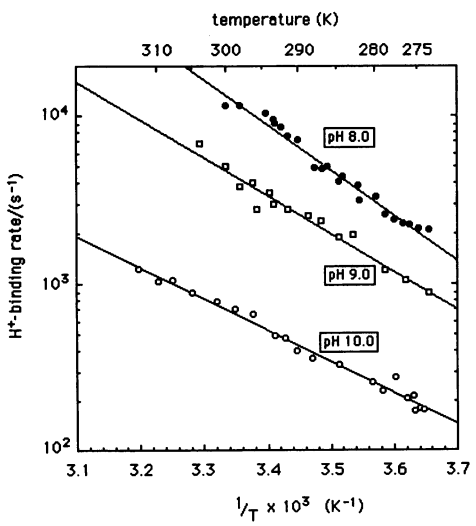

FIGURE 4 Temperature dependence of the H^+ binding rate. Conditions: 100 mM KCl, 0.03% Triton X-100, 60 μM terbutryn, 3.2 μM RC, 40 μM cresol red (●), thymol blue (□), or *o*-cresol phthalein (○). The lines are least-square fits. The calculated activation energies are 0.54 ± 0.03 eV (pH 8.0), 0.45 ± 0.04 eV (pH 9.0), and 0.37 ± 0.03 eV (pH 10.0), and are not corrected for the minor effect of viscosity change (see Fig. 5).

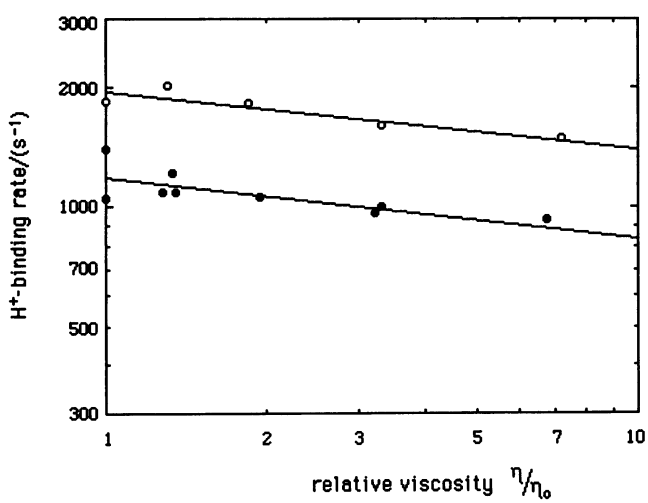

FIGURE 5 Viscosity dependence of the H^+ binding rate. Conditions: 3 μM RC, 60 μM terbutryn, pH 10.0, 293 K; the viscosity (η) was modified by the addition of glycerol; η_o = viscosity of water. Spectrophotometric assay (●): 100 mM KCl, 40 μM *o*-cresol phthalein, 0.03% Triton X-100. Conductimetric assay (○): 20–20 mM ethylenediamine and glycine as buffer pair, 0.06% Triton X-100. Note both scales are logarithmic.

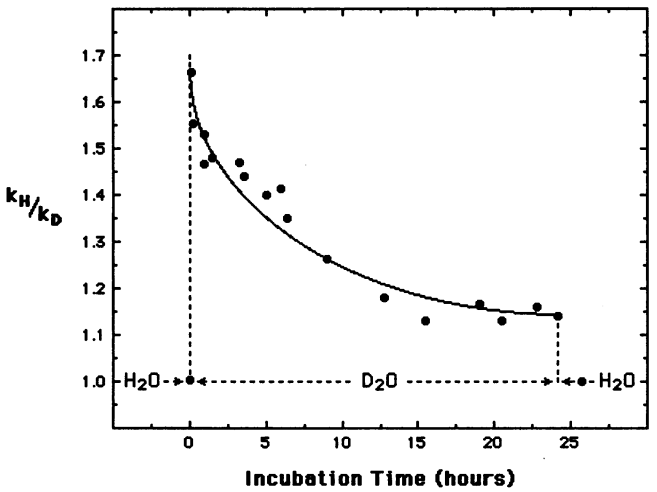

FIGURE 6 Time course of the effect of D_2O on the H^+ (D^+) binding rate. The proton → deuterium exchange was initiated at $t = 0$ by injecting the RC into D_2O. The reaction mixture was split into two equal parts and CAPS, in powdered form, was added to one of them to give a final buffer concentration of 20 mM. The reverse (deuterium → proton) substitution was started after 24 h incubation time by repeated dilution and ultrafiltration in H_2O. At the end of the ultrafiltration (~2 h), the D_2O content of the sample was less than 5%. Conditions: as for Fig. 4, with 3 μM RC, 40 μM indicator dye (thymol blue or *o*-cresol phthalein), pH 10.0 (pD 10.4), and 23°C.

is negligible. This does not support the idea that the kinetics are diffusion controlled. Earlier work showed that the rates of H^+ binding and electron transfer by RCs with functional Q_B (i.e., allowing formation of $P^+Q_B^-$) also exhibit a rather flat pH dependence (Wraight, 1979; Verméglio, 1982). Similar behavior is seen in chromatophores from both *Chromatium vinosum* (Chance et al., 1970) and *Rb. sphaeroides* (Petty et al., 1979), where substantial activation energies as well as very weak viscosity effects were determined. Although these earlier measurements correspond to the formation of $P^+Q_B^-$, the electron transfer between the quinones was not considered rate limiting.

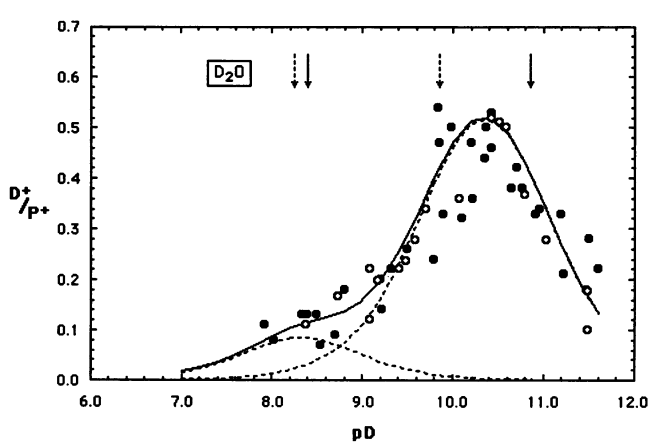

FIGURE 7 D^+ binding stoichiometry versus pD. Conditions: as for Fig. 4, with 1.7 μM RC, and 40 μM pD-indicator dye, depending on the pD, as in Fig 1. D^+ uptake was measured after short (0–2 h, ○) and long (24 h, ●) incubation of the RCs in D_2O. The curves are drawn assuming two noninteracting protonatable groups with dark (PQ_A, ⇢) pK values of 9.85 and 8.25, and light ($P^+Q_A^-$, →) pK values of 10.85 and 8.4.

Mechanisms underlying the observation of H^+ binding by reaction centers

Rate constants for simple acid-base reactions in aqueous solution are in the range 10^{10}-10^{11} M^{-1} s^{-1}, the fastest corresponding to the reaction $H^+ + OH^- \rightarrow H_2O$ ($k_H = 1.3 \times 10^{11}$ M^{-1} s^{-1}; Eigen and de Maeyer, 1955). Values of 2–6 × 10^{10} M^{-1} s^{-1} are commonly found for neutralization of other strong bases (Eigen, 1964; Barker and Sammon, 1967; Bell, 1973; Gutman and Nachliel, 1990). A small extrapolation of our data (Fig. 1 *A*) to more acidic pH values suggests that the measured values intersect the theoretical line between pH 6 and 6.5, close to the reported isoelectric point of 6.1 for isolated RCs (Prince et al., 1974). However, the rate of proton binding is only weakly pH dependent, and the apparent bimolecular rate constant becomes progressively larger at high pH. High salt concentrations, especially divalent salts, significantly slow down the observed rate of H^+ binding and cause downward shifts in the pK values associated with the H^+ stoichiometries.

These findings support an electrostatic influence on the H^+ binding kinetics, and large apparent rate constants could arise from electrostatic enhancement via the surface pH. The RC protein is, indeed, expected to have a substantial negative surface potential at high pH. However, the observation of proton uptake by the RC is not a simple neutralization process, but is detected as the subsequent deprotonation of a reporter group (BH)—a pH indicator or a buffer in the spectrophotometric and conductimetric assays, respectively. As thoroughly expounded by Gutman and coworkers (Nachliel et al., 1987; Gutman and Nachliel, 1990), such deprotonation is dominated by three distinct pathways, none of which actually involve H^+ ion diffusion per se:

1. Spontaneous deprotonation of the reporter group (dye or buffer, respectively, in optical and conductimetric assays) at a rate given by $k_{off} = k_H \times 10^{-pK}$:

$$BH \underset{k_H}{\overset{k_{off}}{\rightleftarrows}} B^- + H^+ \qquad (2)$$

For $k_H = 4 \times 10^{10}$ M^{-1} s^{-1}, k_{off} will be ≤40 s^{-1} for a weak acid with pK ≥ 9. This is clearly too slow to contribute to the rapid net response we observe.

2. Collisional deprotonation of the protonated reporter group at the pK-shifted site of the flash-activated RC:

$$BH + A^- \rightleftarrows B^- + AH \qquad (3)$$

where AH/A^- represents an ionizable group on the protein. Groups active in H^+ binding are those with shifted pK values, and the H^+ stoichiometries (Figs. 3 and 7) show that the pK shifts are on the order of 1 pH unit or less. Thus all contributing groups have pK values in the range of the

prevailing pH (e.g., ±1 unit) and are 10–90% deprotonated before the flash.

Proton transfer reactions, such as Eq. 3, exhibit diffusion-controlled, bimolecular rate constants of $\sim 10^9$ M^{-1} s^{-1}, provided the difference in pK values between the proton donor and acceptor favors the transfer (Eigen, 1964; Bell, 1973; Gutman and Nachliel, 1990). For a given pH indicator, used over a range of pH ≈ pK ± 0.5, the concentration of HIn^- (= BH) will vary from 30 to 10 μM in our experiments (40 μM total indicator concentration). Thus the observed rate of deprotonation should be $\geq 10^4$ s^{-1} and will decrease by only a factor of 3 for one pH unit increase through the pK region. Such rates are at least as large as any observed here, and larger than those above pH 8. At high pH, indicators (or buffers) with higher pK values are used, decreasing the intrinsic donation capabilities of the reporter group. However, the pKs of the relevant acceptor groups on the RC also increase, so the difference in pK remains roughly constant.

3. Protolysis of H_2O at the RC, followed by diffusion of OH^- to deprotonate HIn^-:

$$H_2O + A^- \underset{k_{OH}}{\overset{k_A}{\rightleftharpoons}} OH^- + AH \qquad (4a)$$

$$OH^- + BH \underset{k_B}{\overset{k_{OH}}{\rightleftharpoons}} H_2O + B^- \qquad (4b)$$

At 55.5 M, H_2O is generally an effective proton donor and can compete with other species, especially when the pK of the acceptor is relatively high. The rate constant for protolysis of water by A^- is given by (Gutman and Nachliel, 1990)

$$k_A = k_{OH} \times 10^{(pK-15.74)} \quad (M^{-1}\ s^{-1}) \qquad (5)$$

(The factor 15.74 comes from the ionization constant of water ($K_w = 10^{-14}$) and the concentration of water, i.e., log $[H_2O]/K_w = 15.74$). The pseudo-first-order rate constant (in s^{-1}) in aqueous solution is $k'_A = k_A \cdot [H_2O] = k_{OH} \times 10^{(pK-14)}$. k_{OH} is $\sim 3 \times 10^{10}$ M^{-1} s^{-1} (Nachliel et al., 1987); so, in the range pH 7–11, k'_A is expected to be 3000 s^{-1} to 3×10^7 s^{-1}, corresponding to acceptor groups (A^-) with pK values similar to the prevailing pH. Thus protolysis of water by flash-activated RCs will produce a rapid OH^- pulse roughly equivalent to the net H^+ uptake stoichiometry of 0.1–0.5 H^+/RC. This will be detected by collisional deprotonation of the indicator, according to Eq. 4b. For $\Delta[OH^-] = [RC] \approx 1$ μM, the rate of proton transfer will be $\sim 10^4$ s^{-1}. Again, therefore, the resultant rate is faster than our measured H^+ binding responses in RCs, over most of the pH range. In well-defined experimental systems, Gutman and colleagues have shown that indicator responses to H^+ and OH^- pulses are complete in a few tens of microseconds in the range pH 7–9 (Gutman et al., 1981, 1983; Nachliel et al., 1987).

We may conclude from this summary that although we initially considered the observed rates of proton binding in RCs to be anomalously fast, in fact proton transfer reactions in solution are not generally limited by diffusion of H^+ or OH^-, and are normally faster than our observations. Furthermore, we note that the large temperature coefficients and the lack of a strong viscosity effect are also indicative of a process that is not diffusion controlled. Instead, we must consider why protonation events in the RC are as slow as they are.

Binding of indicator dyes by isolated reaction centers

Equilibrium chromatography measurements and the effects of RCs on the pK values of various indicators show that RCs bind the main types of indicators used in this study (Table 1). The detergent (Triton X-100), at the levels used here, did not appear to bind the indicators significantly. Because chromatophores also do not bind these indicators (Petty and Dutton, 1976), the binding by isolated RCs is likely due to the detergent-associated membrane-spanning regions of the solubilized RC protein. We have recently shown that ubiquinone-10 partitions more favorably (about fourfold) into the RC-LDAO detergent phase than into pure LDAO micelles, even after correction for micelle size and specific binding at the Q_B site (Shinkarev and Wraight, 1997). Thus some distinction can exist between these detergent phases.

The upward shifts in pK values, seen in the presence of RCs (Table 2), could indicate that the protonated form of the indicators is bound preferentially over the deprotonated species, consistent with the greater polarity and charge of the latter (HIn^- versus In^{2-}). The pK shifts would then imply a 12-fold, 6-fold, and 2.5-fold preference for the protonated forms of thymol blue, cresol red, and bromthymol blue, respectively, in 100 mM NaCl. The different magnitudes for these otherwise similar indicators could arise from electrostatic interactions with the pH-dependent negative charge of the protein, which would suppress the relative binding of In^{2-}.

An electrostatic influence on binding is indeed suggested by the increased stoichiometry of thymol blue bound per RC in high salt (500 mM NaCl) at pH 10.5, where the dominant indicator species is In^{2-}. However, at alkaline pH the significant surface potential for the RC, expected from the net charge (see below), should cause the surface pH to be substantially below that of the bulk phase. This will give rise to an apparent shift in pK for surface-bound indicator without any preferential binding of protonated over unprotonated forms. The pK shift will then be a measure of the difference between the bulk and surface pH values.

At the present time, these potential contributions to the apparent pK shift of indicator in the presence of RCs—preferential binding of the protonated indicator species versus surface pH—cannot be distinguished, and may coexist. In any event, the surface charge and pH are major factors, as indicated by the slowing of the rate of H^+ binding at high salt concentrations and the distinct behavior of mono- and

divalent cations. The latter, especially, reflects an effect via the concentration of mobile ions (including H^+) in the ionic double layer around the RC. In our measurements (indicator:RC ratios of 20–40), both bound and free indicator are present, and the observed behavior is an average, resulting from rapid equilibration of the protonation state throughout the indicator population. Because of the pK shift in the bound population, this fortuitously extends the useful pH range for each indicator.

Nature of the rate-limiting event in H^+ uptake by reaction centers

If the observed kinetics of deprotonation of indicator are not determined by the free diffusion of H^+ or OH^- ions, we might seek to invoke special properties of the bound indicators that are the immediate source of the signals. Measurements of proton release by bacteriorhodopsin, using indicators covalently bound to the protein, have shown that the appearance of protons in the bulk phase is considerably slowed relative to their detection at the surface (Heberle and Dencher, 1992; Nachliel et al., 1996), and such surface effects have been widely espoused by Gutman (Gutman et al., 1983; Gutman and Nachliel, 1995). On this basis, it might be suggested that the slowing down of the H^+ binding by RCs, observed here in response to high salt, could be due to loss of indicator bound to the surface of the RC, so that only the more slowly responding bulk-phase indicators are involved. However, within the limited range of applicability of the method, similar results were obtained by conductance measurements, a technique of seemingly impeccable bulk-phase credentials. Therefore, the rate limitation in the proton binding measurements must be located in or at the RC itself. As discussed below, the substantial salt dependence of the rate of proton binding suggests that the concentration of the proton donor (e.g., protonated indicator, HIn^-) at the surface of the RC is also important in the rate determination. Thus, although the process is not diffusion limited, it may be collisional.

The lack of diffusion control in the H^+ ion uptake process is also supported by the observed temperature and viscosity dependences of the kinetics. Diffusion of small particles, including most ions, is well described by the Stokes-Einstein equation and is not strongly activated ($E_a = 0.08–0.15$ eV), whereas the observed H^+ binding rate has a strong temperature dependence ($E_a > 0.35$ eV; Fig. 4). The unusual mechanisms of transport available to protons (hydrogen-bonded networks, etc.) are not expected to add significantly to the activation energy for net movement of H^+ ions in solution.

H^+ uptake as an accessibility-controlled process

It may seem surprising that H^+ binding ($\tau \geq 50$ μs), in response to the de novo photochemical generation of charges within the RC ($\tau \ll 1$ ns), can be rate limited by anything other than the diffusion of potential proton donors. The propagation of the electric field to the surface of the protein should be almost instantaneous, resulting in pK shifts of many near-surface groups—perhaps as envisaged by McPherson et al. (1988). However, the polarization of the protein environment, and the effective local charge screening around the quinones, could be large and rapid, as part of the functional evolution of these sites. Indeed, recent analysis of the protein response to formation of $P^+Q_A^-$ suggests that the major part of the relaxation ($\approx$ 100 meV) is complete in less than a microsecond (McMahon et al., 1996; Nienhaus et al., 1997). Furthermore, the immediate response to any potential changes at the surface will be very rapidly effected by counter-ion redistribution—predominantly of cations other than protons. The remaining changes in chemical affinity for protons may be more specifically localized on a small number of ionizable groups whose response is controlled by other factors.

That the observed H^+ binding to $P^+Q_A^-$ is not a simple electrostatic response by surface groups is supported by observations on a site-directed RC mutant in which aspartic acid at position 213 of the L-subunit has been replaced by asparagine (Takahashi and Wraight, 1990, 1992). This mutation results in a complete block of the second electron transfer to Q_B, allowing stable formation of the species $Q_A^-Q_B^-$ after the second flash. This state induces very little proton binding (< 0.05 H^+/RC), compared to Q_A^- alone ($\approx$0.3 H^+/RC), even though the instantaneous electric field due to Q_A^- at the protein surface is likely to be similar to that after a single flash. Presumably the specifically protonatable sites are already largely saturated by H^+ ion uptake on the first flash, in response to Q_B^- formation.

Thus we are led to suggest that the H^+ uptake by RCs in the $P^+Q_A^-$ state requires a finite rearrangement between "accessible" and "inaccessible" states that must precede actual H^+ binding or transfer. Because H^+ transfer on these time scales is an essentially adiabatic process, e.g., requiring connectivity of a hydrogen-bonded pathway, this could be a small-amplitude event. The term "conformation," used below, is for convenience only and does not imply a particular magnitude of the motion.

The change between "accessible" and "inaccessible" states could be directly rate limiting, and the pH dependence and activation parameters of proton uptake would then be ad hoc properties of the conformational kinetics. Alternatively, rate control by events within the RC can arise if the conformational equilibrium is fast, viz.:

$$RC^i \underset{\text{fast}}{\overset{K_c}{\longleftrightarrow}} RC^a \xrightarrow{k \cdot f\{BH\}} RCH^+ \qquad (6)$$

Here $K_c = [RC^a]/[RC^i]$ is the equilibrium constant between accessible and inaccessible states of the unprotonated reaction center, after flash excitation. $k \cdot f\{BH\}$ denotes the pseudo-first-order proton transfer rate, where k is the bimolecular rate constant for proton transfer, and $f\{BH\}$ indicates the effective concentration of proton donor (e.g., in-

dicator or buffer) as determined by the surface pH. If the rate of the conformational change is larger than $k \cdot f\{BH\}$, then the observed proton binding rate can be approximated by

$$\text{Rate} = k \cdot f\{BH\} \cdot \frac{K_c}{1 + K_c} \tag{7}$$

The H^+ ion uptake rate is then proportional to a bimolecular rate process, but is multiplied by a factor that is always less than 1. If the conformational equilibrium of Eq. 6 lies far to the left ($K_c \ll 1$), the net rate will be significantly below the diffusion limit, and the free energy of the conformational change will contribute significantly to the apparent activation energy for H^+ binding.

The very weak viscosity dependence of the H^+ binding kinetics is not obviously consistent with a collisional reaction, whether diffusion limited or not. However, the viscosity dependence is complex, and at the present time, we are unable to incorporate this behavior into a coherent framework of the reaction. As described below, the H^+ binding reaction exhibits strong influences from surface properties, and the indicator itself is partially surface bound. This may restrict the extent to which low values of bulk-phase viscosity can affect the reaction kinetics, and the drastic affect at higher viscosities may reflect glycerol effects on the surface, including bound water structures (Gekko and Timasheff, 1981), rather than a viscosity effect per se.

It is noteworthy that the equilibrium form of Eq. 6 can also describe the effect of solvent exclusion on the pK of a buried residue, i.e.,

$$\begin{array}{ccc} RC^i & \overset{pK^i}{\longleftrightarrow} & RC^iH^+ \\ {\scriptstyle K_c}\updownarrow & & \updownarrow{\scriptstyle K_c'} \\ RC^a & \underset{pK^a}{\longleftrightarrow} & RC^aH^+ \end{array} \tag{8}$$

where pK^i and pK^a refer to inaccessible (occluded) and solvent-accessible situations, and K_c and K_c' describe the equilibrium between these conformations in the unprotonated and protonated states, respectively. The observed pK is given by

$$pK^{obs} = pK^a - \log K_c/K_c' \tag{9}$$

Thus pK^{obs} can be significantly different from pK^a, depending on the relative values of K_c' and K_c. Given the overwhelming importance of electrostatics in this situation, the more favorable conformational equilibrium will be that for the neutral state of the buried residue. For example, in the Q_B binding pocket, an apparent pK of 9.6 is associated with Glu^{L212} (Paddock et al., 1989; Takahashi and Wraight, 1992), although this functional pK may also involve other carboxylic acid residues (Gunner and Honig, 1992; Beroza et al., 1995; Lancaster et al., 1996). Some of this large pK shift is undoubtedly due to electrostatic interactions with nearby residues, but much should be attributable to its total occlusion from the bulk solvent, and computational analyses of this system do support a significantly shifted value for the intrinsic pK of this residue (Gunner and Honig, 1992; Beroza et al., 1995). (An intrinsic pK is the value that would be obtained for the "discharged" state of the protein, where all ionizable residues, other than that being titrated, are neutral. In most cases, this is similar to the solution value, reflecting the contributions of dipoles inside the protein, but for some buried residues it can be very far removed.)

Glu^{L212} has been strongly implicated as a site of proton binding in response to reduction of the secondary quinone (i.e., Q_B^-) at high pH (>9) (Paddock et al., 1989; Takahashi and Wraight, 1992). However, substantial evidence exists to suggest that Glu^{L212}, and possibly other residues in the Q_B binding domain, is selectively protonated in response to Q_A^- as well as Q_B^-. This would imply long-range interactions (>15 Å) between Q_A^- and the Q_B pocket, of an apparently electrostatic nature (Sebban et al., 1995). Most notably, mutation of Glu^{L212}, in the very closely related species, *Rb. capsulatus*, eliminates H^+ binding by Q_A^- above pH 9 (Maróti et al., 1995; Miksovska et al., 1996), strongly supporting a role for this residue in proton binding. Interactions between the Q_A and Q_B binding sites have long been indicated by differential effects of the occupant of the Q_B site on the protonation and redox properties of Q_A (Prince and Dutton, 1978; Wraight, 1981, 1982).

Electrical measurements on RCs in lipid bilayers have revealed a small component of electrogenesis associated with Q_A reduction (i.e., independent of the presence of Q_B), occurring on the same time scale as the proton binding reported here (Brzezinski et al., 1992). However, the sign of the voltage change was opposite that expected for proton transfer from the aqueous phase, and it was interpreted to reflect movement of an internal charge, such as an internal ionizable amino acid residue. This component was absent in mutant RCs with Glu^{L212} changed to Gln by site-directed mutagenesis. It was suggested that the motion implied by the electrogenicity might be a precursor for electron transfer to Q_B. It could also correspond to the "accessibility gate," proposed here, for protonating internal residues. The occurrence of significant structural changes in the functioning of the quinone acceptors has been suggested by x-ray diffraction studies, which show a substantial difference in the position of Q_B in dark-adapted and preilluminated samples (Stowell et al., 1997).

The role of surface properties in the H^+-binding behavior

Although the rate limitation to proton uptake appears to be localized within the RC, the salt dependence of the kinetics of the indicator response, at a fixed bulk phase pH, implies an involvement of the surface pH, as determined by the surface potential and charge of the RC. The indicators used showed upward shifts in pK upon association with the RC, consistent with a significantly lower pH at the protein surface than in the bulk phase, as would arise from a

substantial net negative charge. This is as expected from the isoelectric point of the protein (pI ≈ 6.1; Prince et al., 1974) and from its amino acid content. High salt decreased the RC-induced shifts in indicator pKs, as expected for a relative increase in the surface pH due to suppression of the surface potential. This will cause a decrease in the surface concentration of protonated indicator, which, in turn, results in slower kinetics of any process involving HIn^- as a proton donor in a bimolecular reaction.

A rough description of these surface potential effects can be made using Gouy-Chapman theory—which approximates the RC as an infinite planar sheet! This may seem to be of doubtful applicability, but Gouy-Chapman theory is known to be extraordinarily robust in geometric and surface approximations (McLaughlin, 1989; Israelachvili, 1992). The integrated one-dimensional Poisson-Boltzmann equation at the surface of the protein, approximated by a plane, is given by the Grahame equation (Barber, 1980):

$$\frac{\sigma^2}{2\epsilon_r\epsilon_o RT} = \sum a_i[\exp(-z_i F\psi_o/RT) - 1] \qquad (10a)$$

where σ is the surface charge density and ψ_o is the electrostatic potential of the surface relative to the potential of the bulk phase. T denotes the temperature; ϵ_r and ϵ_o are the relative dielectric constant of the medium (taken as 80 for bulk water) and the permittivity of a vacuum, respectively; R is the gas constant; F is the Faraday constant; z_i is the charge carried by the ith ion; and a_i is its activity, which can be expressed in terms of an activity coefficient, $a_i = f_i \cdot c_i$, where f_i may be derived from Debye-Hückel theory: $\log f_i = -0.509 z_i\sqrt{I} + bI$. I is the ionic strength of the solution, with its usual definition, $I = 0.5\Sigma c_i z_i^2$, and b is an empirical constant. The ions throughout the aqueous phase follow a Boltzmann-type distribution in the electric field, generated by the surface charge on the protein and by the mobile ions themselves.

As the Poisson-Boltzmann equation cannot be integrated in the limit of zero ionic strength, a background (residual) ionic content of the solution must be assumed:

$$\frac{\sigma^2}{2\epsilon_r\epsilon_o RT} = \sum a_a[\exp(-z_a F\psi_o/RT) - 1] + \sum a_b[\exp(-z_b F\psi_o/RT) - 1] \qquad (10b)$$

where z_a, z_b and a_a, a_b denote the charge and the activity of the added (subscript a) and background (subscript b) ions, respectively. The first term on the right-hand side of Eq. 10b includes the contribution of all the ions externally titrated into the solution.

Mobile ions distribute in the electric field of the diffuse layer adjacent to the charged surface of the protein. Because of their small concentration relative to that of other ions, H^+ ions do not modify the electric field in the same way as other ions in the diffuse layer, but only sense it. However, their involvement in protonation equilibria of ionizable residues can modify the surface charge directly, and hence substantially influence the surface potential. The H^+ ion equilibrium concentration at the surface of the RC, $[H^+]_s$, relative to that of the bulk volume, $[H^+]_v$, is governed entirely by the surface potential:

$$\frac{[H^+]_s}{[H^+]_v} = \exp(-F\psi_o/RT) \qquad (11a)$$

$$pH_s = pH_v + F\psi_o/2.3RT \qquad (11b)$$

Thus, through ψ_o, unscreened negative charges on the surface of the RC increase the local H^+ ion concentration and, hence, decrease the local (surface) pH.

The divalent cation, Mg^{2+}, was effective at concentrations more than two orders of magnitude smaller than the monovalent cation, K^+ (Fig. 2 *A*). This large difference would indicate a very substantial surface potential and charge density if the effect on the rate were directly through the surface pH (rate ≈ $k[H^+]_s$), i.e., by Eqs. 10 and 11, alone. The data can be adequately described this way, but the fit is very sensitive to the presumed background concentration of ions and requires unreasonably high values: $c_b' = 5 \times 10^{-2}$ M monovalent or $c_b'' = 3 \times 10^{-4}$ M divalent salts (symmetrical salts were assumed for convenience, with a negligible effect on the numerical outcome). Direct conductance measurements showed the sample preparation procedure, including pH adjustment and counterions for the RCs and added indicator, to result in ionic concentrations of ~100 μM, and almost all of this is expected to be monovalent salt.

Following the discussion of proton transfer mechanisms, above, we suppose that the observed H^+ binding rate is proportional to the concentration of some protonated species near the site of protonation, according to the local (surface) pH (pH_s). In the optical assay of proton uptake, the immediate proton donor is likely to be bound indicator, HIn^-, as this is the dominant buffering species present, but in other conditions it will be different species, such as added buffer in the conductance assay. Morover, in general, both donor and acceptor species will change identity as the prevailing pH changes. pH_s is determined by the bulk volume pH (pH_v) and the surface potential, through the exponential term of Eq. 10. Thus $f\{BH\}$ in Eq. 7 is the surface concentration, $[BH]_s$, and

$$k[BH]s = \frac{k[B_0]}{1 + 10^{pH_s - pK}} = \frac{k[B_0]}{1 + 10^{pH_v - pK + \psi_0 F/(2.3RT)}} \qquad (12)$$

where k is the bimolecular rate constant for proton transfer from the proton donor (BH). This is expected to be on the order of 10^9 M^{-1} s^{-1}, if unrestricted by any other process. B_o is the total donor or buffer concentration, and the pK refers to the donor species (BH/B^-).

The salt dependence of the H^+ ion-binding rate, at pH 10.0, was simulated by numerical solution of the Grahame equation (Eq. 10), assuming fixed surface charge density, and inserting the calculated value of ψ_o into Eq. 12. With

this approach the fit is very insensitive to the background ionic concentration. If the total ion concentration is very low, pH_s is also low, and the donor is fully protonated. The rate of proton transfer is then at maximum and remains constant until the added salt is high enough to affect the surface pH in the range of the donor pK. Thus the background salt concentration need be specified only to make the surface pH realistic.

With this model, the pK of the donor and the charge density compensate each other to give good fits in the range $pK = 8.2 \pm 0.2$ (at infinite ionic strength) and $\sigma = -0.7 \pm 0.2$ q/nm^2, with background ionic concentrations of 100 μM monovalent and 5–10 μM divalent salts (assumed symmetrical), both acceptable values. The charge density obtained is somewhat high, but includes a contribution from the bound indicator, and seems feasible for a relatively local value, considering the large number and highly clustered distribution of charge residues in the H-subunit (Zhu and Karlin, 1996).

The bimolecular rate constant, k (Eq. 12), is determined by the rate in the plateau region at low salt, where $pH_s < pK$ of the donor species, and is independent of any parameters of the fit to the data. From the observed rate of 1.6×10^3 s^{-1}, and using the total added indicator concentration (40 μM) as a lower limit for B_o in Eq. 12, we obtain $k = 4 \times 10^7$ M^{-1} s^{-1}. For a good donor species, like an oxy-acid or indicator, k is expected to be $1–5 \times 10^9$ M^{-1} s^{-1} (Eigen, 1964; Gutman and Nachliel, 1990). Comparison of these two values suggests a possible magnitude of the conformational factor in Eq. 7, leading to $K_c \leq 10^{-2}$. If the comparison is appropriate, this provides a quantitative assessment of the degree of inaccessibility of the protonation site within the RC.

Deviations from expectation

For the monovalent cation titration, especially, the data diverge from the simple theoretical expectations at high salt concentration. This is entirely reasonable under the assumption of fixed surface charge. The net charge on the protein is quite negative at pH 10, giving rise to a substantial lowering of the surface pH relative to the bulk. As the salt concentration is increased, pH_s will increase, leading to further dissociation of protonated surface residues and an increase in the net charge density. This will partly counteract the screening effect of the added salt, causing deviations from the expected decrease in surface potential. The greater divergence in the KCl than in the $MgCl_2$ titration is consistent with this, as the model shows pH_s to increase more over the range of KCl concentrations (Fig. 2 *B*). In fact, the pH_s values encountered here are initially in a range (pH 7–8.5) where the surface charge is relatively insensitive to pH because of the low probability of functional pK values for surface ionizable amino acid side chains (carboxylate $pK < 4.5$; histidinyl $pK < 7$; amino and tyrosyl $pKs > 9$; guanidinium $pK > 11$). This undoubtedly contributes to the success of the model, with the fixed charge approximation.

Adsorption of cations to the protein can also perturb the charge density, but this should be similar over the course of the two titrations, because any greater affinity for divalent Mg^{2+} will be mitigated by the lower concentrations used. In contrast, any effects of anion (Cl^-) binding, which would lead to relatively more negative surface charge, will not be the same because of the higher concentrations (up to 1 M) in the KCl compared to the $MgCl_2$ titration (<10 mM). This, too, may contribute to the larger deviation in the monovalent salt titration.

Given the approximations involved, the precise values of the parameters used (which are reasonable) are not as significant as the general shape and satisfactory fit to both salt curves with a single parameter set (Fig. 2 *A*). Nevertheless, there must be some fortuity in this fit, as the surface charge of the RC certainly becomes more negative at high salt as the surface pH increases. A more sophisticated analysis would include ionization of specific residues, as well as binding of ions at high salt concentrations. A necessary prerequisite for this, however, is calculation of the effective pK values of all of the ionizable residues of the RC. Structure-based approaches to electrostatic calculations for RCs are currently being developed (Gunner and Honig, 1992; Beroza et al., 1991, 1992, 1995; Lancaster et al., 1996) and are likely to be useful in the not too distant future.

pH dependence of the H^+ binding kinetics

The conclusion that diffusion of H^+ ions does not limit the observed H^+ binding kinetics leads to the expectation that the rate will be roughly pH independent. Even if the rate limitation were in the bimolecular reaction with surface-bound, protonated indicator, the use of different indicators (with appropriately varied pK values to match the experimental pH) would keep the relative amounts of protonated and unprotonated species roughly constant over a wide pH range. The rate of proton uptake was not significantly dependent on the concentration of total indicator, which may seem to rule out the protonated indicator as the primary proton donor. However, the binding studies showed that the binding of indicator by RCs was easily saturated at the concentrations used. Thus the effective concentration of protonated indicator at the surface is not readily manipulatable through the bulk concentration, although it is varied by the (surface) pH. Consequently, some small decline in rate (up to threefold per pH unit) might be expected over the range of pH applied to any one indicator, but the origin of the finite slope over the whole pH range, encompassing many indicators, is not known. It may stem from the lower amounts of bound indicator at high pH (Table 1), from a steady decrease in the proton-donating potential of donors, including indicators, with higher pKs, or from some property intrinsic to the RC.

Isotope effects

Replacement of H_2O by D_2O, and the subsequent exchange of acidic and basic protons, gives rise to so-called solvent isotope effects, including primary, secondary, and "solvation" or "transfer" effects (Bell, 1973; Klinman, 1977; Schowen and Schowen, 1982). The effects of deuterium exchange in D_2O on certain electron transfer events in RCs have been investigated previously (Schenck et al., 1982; Okamura and Feher, 1986). Isotope effects on rates of electron transfer have generally been interpreted as arising from modified skeletal vibrations of the protein. As the coupling of electron transfer to the vibrational modes is generally not strong, the isotope effect is usually small (a few percent). In proton transfer reactions, much larger changes can sometimes be seen if the transferring species itself is isotopically exchanged. However, proton transfer between strong acids and bases rarely exhibits large isotope effects. The deuterium solvent isotope effect on the rate of H^+ (D^+) binding by RCs (k_H/k_D) is quite typical of many biochemical reactions (Klinman, 1977). At pH (pD) 10.0, the deuterium ion binding rate is about half that of the proton binding rate, and the data suggest that a maximum effect of about 3 may be reached at higher pH (Fig. 2 *C*).

From the data of Fig. 5, doubling the viscosity of the solution from 1 to 2 cp decreased the rate by ~15%. Because the macroscopic viscosity of D_2O at 25°C is 25% greater than that of H_2O (Schowen and Schowen, 1982), ~4% of the effect of deuterium exchange on the H^+ (D^+) binding rate can be ascribed to the change in viscosity. Measurements of diffusion-controlled reaction rates tend to indicate larger differences (1.8–2.2-fold) in the diffusion limit for small molecules in D_2O compared with H_2O (Pines et al., 1986). If this reflects a microviscosity, possibly relevant to the RC protein fluctuations, then a potentially more significant, but still minor, fraction (<20%) of the prompt effect of D_2O substitution might be attributable to the weak viscosity dependence. In either case, this would come under the category of a "solvation" and/or "transfer" isotope effect of D_2O.

In addition to the "solvation" isotope effect, the prompt effects seen when RCs were injected into D_2O could arise from 1) a primary kinetic isotope effect, due to substitution of H^+ by D^+ at the bond that is affected in the protonation reaction; 2) secondary kinetic isotope effects, due to isotopic substitution in other parts of the protein not directly involved in the H^+ (D^+) binding/unbinding, or a combination of these contributions. However, we have concluded that the H^+ (D^+) binding is rate limited by conformational events in the protein, rather than being diffusion controlled, and the substantial activation energy for both H^+ and D^+ binding supports this. Thus any primary isotope effect that might occur in the H^+ transfer per se would be masked by the rate limitation residing in other steps of the overall process, and the measured isotope effect is not mechanistically revealing.

In fact, the kinetic effects of D_2O exchange are probably accountable in terms of equilibrium isotope effects, as indicated by the H^+ (D^+) binding stoichiometries. The distinct isotope-induced pK shifts for proton binding by RCs (+0.1–0.3; Table 3) are similar to those seen for primary equilibrium isotope effects on simple acid-base equilibria in pure H_2O and D_2O, which are in the range of ΔpK = 0.2–0.8, e.g., 0.40–0.65 for oxy-acids and 0.30–0.40 for thiol acids (Bell, 1973). Such primary effects are mainly determined by the stretching and bending frequencies of the X–H bond (Bell, 1973; Klinman, 1977). Secondary isotope effects are usually much smaller. However, in the context of Eq. 8, whereby functional pK values are controlled by accessibility, a primary effect on the conformational equilibrium would have an equal (secondary) effect on the pK. Thus the isotope shift of 0.3 pK units observed for the light pK of group 1 (see Table 3) would reflect a twofold change in the conformational equilibrium, consistent with the decrease by a factor of 2 in the rate of proton uptake, at pH 10, according to Eq. 7. The very small isotope shift (0.1 pK units) for the light pK of group 2 is also consistent with the negligible kinetic isotope effect at pH 8.

In the long-term D_2O incubation experiments, the rate of D^+ binding increases again (i.e., an inverse effect), almost reaching the rate of H^+ binding observed in H_2O. This implies a secondary isotope effect associated with deuteration of buried groups. Such slow exchange is common for peptide nitrogens involved in secondary structure (Englander and Kallenbach, 1984) and may be dependent on, and may possibly induce, structural changes not directly related to the flash-induced protonatable groups, e.g., breaking hydrogen bonds in the protein (Klinman, 1977; Schowen and Schowen, 1982). It is interesting to note that the isotope effect on the $P^+Q_A^-$ recombination reaction, described by Okamura and Feher (1986), is also an inverse one, with $k_H/k_D \approx 0.94$, and the half-time for exchange in D_2O was ~2 h. This appeared to be a specific effect identified, by ENDOR, with exchangeable sites in direct contact with the quinone.

CONCLUSIONS

The fast kinetics of H^+ binding by RCs in the $P^+Q_A^-$ state, seen at high pH, yield an apparent bimolecular rate constant that is improbably large. Consideration of the events leading to the observed deprotonation of the reporter group (pH indicator or bulk phase buffer) shows that the limiting process is not the diffusion of protons or any proton-carrying species, but more likely an event within the reaction center. Accordingly, the pH, temperature, viscosity, and isotope dependences of the rate are not as expected for a diffusion-controlled reaction. The kinetics of proton binding by RCs were interpreted in terms of accessibility factors for protonation at or within the protein. If this is correct, it is unlikely that any substantial portion of the net proton binding, in the range pH 8–11, could arise from a general

response distributed widely over many solvent-accessible residues. Restricted accessibility seems more likely to be a local property, appropriate only for buried residues, and recent mutational studies have implicated Glu^{L212} in the Q_B binding pocket as a likely protonation site (Maróti et al., 1995; Miksovska et al., 1996). This would imply a degree of focusing of the energetic influences of the semiquinone anion onto a select group of residues, possibly involving dynamic responses to the light-induced charges that are not readily incorporated into existing computational methods.

The authors are grateful to M. R. Gunner (City College, New York) and V. P. Shinkarev (Urbana, IL) for useful discussions. We are especially indebted to M. Gutman (Tel Aviv, Israel) for a clear exposition of the alternative pathways leading to observation of H^+ binding events, and to W. Junge (Osnabrück, Germany) and S. McLaughlin (Stonybrook, NY) for their helpful comments on this work.

This work was supported by grants from the National Science Foundation to CAW (MCB92-08249 and 96-31063).

REFERENCES

Barber, J. 1980. Membrane surface charges and potential in relation to photosynthesis. *Biochim. Biophys. Acta.* 594:253–308.

Barker, G. C., and D. C. Sammon. 1967. Kinetics of proton-transfer reactions. *Nature.* 213:65–66.

Bell, R. P. 1973. The Proton in Chemistry, 2nd Ed. Cornell University Press, New York.

Beroza, P., D. R. Fredkin, M. Y. Okamura, and G. Feher. 1991. Protonation of interacting residues in a protein by a Monte Carlo method: application to lysozyme and the photosynthetic reaction center. *Proc. Natl. Acad. Sci. USA.* 88:5804–5808.

Beroza, P., D. R. Fredkin, M. Y. Okamura, and G. Feher. 1992. Proton transfer pathways in reaction centers of *Rhodobacter sphaeroides:* a computational study. *In* The Photosynthetic Bacterial Reaction Center. II. Structure, Spectroscopy and Dynamics. J. Breton and A. Verméglio, editors. Plenum Press, New York. 363–374.

Beroza, P., D. R. Fredkin, M. Y. Okamura, and G. Feher. 1995. Electrostatic calculations of amino acid titration and electron transfer, $Q_A^-Q_B \rightarrow Q_AQ_B^-$, in the reaction center. *Biophys. J.* 68:2233–2250.

Brzezinski, P., M. Y. Okamura, and G. Feher. 1992. Structural changes following the formation of $D^+Q_A^-$ in bacterial reaction centers: measurement of light-induced electrogenic events in RCs incorporated in a phospholipid monolayer. *In* The Photosynthetic Bacterial Reaction Center. II. Structure, Spectroscopy and Dynamics. J. Breton and A. Verméglio, editors. Plenum Press, New York. 321–330.

Chance, B., A. R. Crofts, M. Nishimura, and B. Price. 1970. Fast membrane H^+ binding in the light-activated state of *Chromatium* chromatophores. *Eur. J. Biochem.* 13:364–374.

Drachev, L. A., M. D. Mamedov, A. Yu. Mulkidjanian, A. Yu. Semenov, V. P. Shinkarev, and M. I. Verkhovsky. 1990. Electrogenesis associated with proton transfer in the reaction center protein of the purple bacterium *Rhodobacter sphaeroides. FEBS Lett.* 259:324–326.

Eigen, M. 1964. Proton transfer, acid-base catalysis, and enzymatic hydrolysis. Part I. Elementary processes. *Angew. Chem. Int. Ed. Engl.* 3:1–72.

Eigen, M., and L. C. M. de Maeyer. 1955. Untersuchungen über die Kinetik der Neutralisation. I. *Z. Elektrochem.* 59:986–993.

Englander, S. W., and N. R. Kallenbach. 1984. Hydrogen exchange and structural dynamics of proteins and nucleic acids. *Q. Rev. Biophys.* 16:521–655.

Gekko, K., and S. N. Timasheff. 1981. Thermodynamic and kinetic examination of protein stabilization by glycerol. *Biochemistry.* 20: 4677–4686.

Glasoe, P. K., and F. A. Long. 1960. Use of glass electrodes to measure acidities in deuterium oxide. *J. Phys. Chem.* 64:188–190.

Graige, M. S., M. L. Paddock, J. M. Bruce, G. Feher, and M. Y. Okamura. 1996. Mechanism of proton-coupled electron transfer for quinone (Q_B) reduction in reaction centers of *Rb. sphaeroides. J. Am. Chem. Soc.* 118:9005–9016.

Gunner, M. R., and B. Honig. 1992. Calculation of proton uptake in *Rhodobacter sphaeroides* reaction centers. *In* The Photosynthetic Bacterial Reaction Center. II. Structure, Spectroscopy and Dynamics. J. Breton and A. Verméglio, editors. Plenum Press, New York. 403–410.

Gutman, M., D. Huppert, E. Pines, and E. Nachliel. 1981. Probing the micelle/water interface by a rapid laser-induced proton pulse. *Biochim. Biophys. Acta.* 642:15–26.

Gutman, M., and E. Nachliel. 1990. The dynamic aspects of proton transfer processes. *Biochim. Biophys. Acta.* 1015:391–414.

Gutman, M., and E. Nachliel. 1995. The dynamics of proton exchange between bulk and surface groups. *Biochim. Biophys. Acta.* 1231: 123–138.

Gutman, M., E. Nachliel, E. Gershon, and R. Giniger. 1983. Kinetic analysis of the protonation of a surface group of a macromolecule. *Eur. J. Biochem.* 134:63–69.

Heberle, J., and N. Dencher. 1992. Surface-bound optical probes monitor proton translocation and surface potential changes during the bacteriorhodopsin photocycle. *Proc. Natl. Acad. Sci. USA.* 89:5996–6000.

Israelachvili, J. 1992. Intermolecular and Surface Forces, 2nd Ed. Academic Press, San Diego.

Kleinfeld, D., M. Y. Okamura, and G. Feher. 1984. Electron transfer in reaction centers of *Rhodopseudomonas sphaeroides.* I. Determination of the charge recombination pathway of $D^+Q_AQ_B^-$ and free energy between $Q_A^-Q_B$ and $Q_AQ_B^-$. *Biochim. Biophys. Acta.* 766:126–140.

Kleinfeld, D., M. Y. Okamura, and G. Feher. 1985. Electron transfer in reaction centers of *Rhodopseudomonas sphaeroides.* II. Free energy and kinetic relations between the acceptor states $Q_A^-Q_B^-$ and $Q_AQ_B^{2-}$. *Biochim. Biophys. Acta.* 809:291–310.

Klinman, J. P. 1977. Kinetic isotope effects in enzymology. *Adv. Enzymol.* 46:415–494.

Lancaster, C. R. D., H. Michel, B. Honig, and M. R. Gunner. 1996. Calculated coupling of electron and proton transfer in the photosynthetic reaction center of *Rhodopseudomonas viridis. Biophys. J.* 70: 2469–2492.

Maróti, P., D. K. Hanson, M. Schiffer, and P. Sebban. 1995. Long range electrostatic interaction in the bacterial photosynthetic reaction center. *Nature Struct. Biol.* 2:1057–1059.

Maróti, P., and C. A. Wraight. 1988a. Flash-induced H^+ binding by bacterial photosynthetic reaction centers: comparison of spectrophotometric and conductimetric measurements. *Biochim. Biophys. Acta.* 934: 314–328.

Maróti, P., and C. A. Wraight. 1988b. Flash-induced H^+ binding by bacterial photosynthetic reaction centers: influences of the redox states of the acceptor quinones and primary donor. *Biochim. Biophys. Acta.* 934:329–347.

Maróti, P., and C. A. Wraight. 1989a. Kinetic correlation between electron transfer and H^+ binding in reaction centers of the photosynthetic bacterium *Rb. sphaeroides. Biophys. J.* 55:182a.

Maróti, P., and C. A. Wraight. 1989b. Anomalous kinetics of flash-induced H^+ ion binding in reaction centers from *Rb. sphaeroides. Biophys. J.* 55:428a.

Maróti, P., and C. A. Wraight. 1990. Kinetic correlation between H^+ binding, semiquinone disappearance and quinol formation in reaction centers of *Rb. sphaeroides. In* Current Research in Photosynthesis, Vol. 1. M. Baltscheffsky, editor. Kluwer Academic Publishers, Dordrecht, The Netherlands. 165–168.

McLaughlin, S. 1989. The electrostatic properties of membranes. *Annu. Rev. Biophys. Biophys. Chem.* 18:113–136.

McMahon, B., J. D. Müller, C. A. Wraight, and G. U. Nienhaus. 1996. Electron transfer and structural relaxations in reaction centers. *Biophys. J.* 72:A418.

McPherson, P. H., M. Y. Okamura, and G. Feher. 1988. Light-induced proton uptake by photosynthetic reaction centers from *Rhodobacter sphaeroides* R-26. I. Protonation of the one-electron states, $D^+Q_A^-$, DQ_A^-, $D^+Q_AQ_B^-$ and $DQ_AQ_B^-$. *Biochim. Biophys. Acta.* 934:348–368.

Mikkelsen, K., and S. O. Nielsen. 1960. Acidity measurements with the glass electrode in H_2O-D_2O mixtures. *J. Phys. Chem.* 64:632–637.

Miksovska, J., P. Maróti, J. Tandori, M. Schiffer, D. K. Hanson, and P. Sebban. 1996. Distant electrostatic interactions modulate the free energy level of Q_A^- in the photosynthetic reaction center. *Biochemistry.* 35: 15411–15417.

Nachliel, E., M. Gutman, S. Kiryati, and N. A. Dencher. 1996. Protonation dynamics of the extracellular and cytoplasmic surface of bacteriorhodopsin in the purple membrane. *Proc. Natl. Acad. Sci. USA.* 93: 10747–10752.

Nachliel, E., Z. Ophir, and M. Gutman. 1987. Kinetic analysis of fast alkalization transient by photoexcited heterocyclic compounds: pOH jump. *J. Am. Chem. Soc.* 109:1342–1345.

Nienhaus, G. U., B. H. McMahon, J. D. Müller, and C. A. Wraight 1997. Protein dynamics from intramolecular electron transfer. *In* Glasses and Glass-Formers, Current Issues. C. A. Angell, T. Egami, J. Kieffer, G. U. Nienhaus, K. L. Ngai, editors. MRS Publications, Pittsburgh, PA. In press.

Okamura, M. Y., and G. Feher. 1986. Isotope effect on electron transfer in reaction centers from *Rhodopseudomonas sphaeroides. Proc. Natl. Acad. Sci. USA.* 83:8152–8156.

Okamura, M. Y., and G. Feher. 1992. Proton transfer in reaction centers from photosynthetic bacteria. *Annu. Rev. Biochem.* 61:861–896.

Okamura, M. Y., and G. Feher. 1995. Proton-coupled electron transfer reactions of Q_B in reaction centers from photosynthetic bacteria. *In* Anoxygenic Photosynthetic Bacteria. R. E. Blankenship, M. T. Madigan, and C. E. Bauer, editors. Kluwer Academic Publishers, Dordrecht, The Netherlands. 577–594.

Paddock, M. L., M. Y. Okamura, and G. Feher. 1989. Pathway of proton transfer in bacterial reaction centers: Replacement of glutamic acid 212 in the L-subunit by glutamine inhibits quinone (secondary acceptor) turnover. *Proc. Natl. Acad. Sci. USA.* 86:6602–6606.

Paddock, M. L., P. H. McPherson, M. Y. Okamura, and G. Feher. 1990. Pathway of proton transfer in bacterial reaction centers: replacement of serine-L223 by alanine inhibits electron and proton transfers associated with reduction of quinone to dihydroquinone. *Proc. Natl. Acad. Sci. USA.* 87:6803–6807.

Petty, K. M., and P. L. Dutton. 1976. Properties of the flash-induced proton binding encountered in membranes of *Rps. sphaeroides*: a functional pK on the ubisemiquinone? *Arch. Biochem. Biophys.* 172:335–345.

Petty, K. M., J. B. Jackson, and P. L. Dutton. 1979. Factors controlling the binding of two protons per electron transferred through the ubiquinone and cytochrome b/c_2 segment of *Rhodopseudomonas sphaeroides* chromatophores. *Biochim. Biophys. Acta.* 546:17–42.

Pines, E., D. Huppert, M. Gutman, N. Nachliel, and M. Fishman. 1986. The pOH jump: determination of deprotonation rates of water by 6-methoxyquinoline and acridine. *J. Phys. Chem.* 90:6366–6370.

Prince, R. C., R. J. Cogdell, and A. R. Crofts. 1974. The photooxidation of horse heart cytochrome *c* and native cytochrome c_2 by reaction centers from *Rhodopseudomonas spheroides* R_{26}. *Biochim. Biophys. Acta.* 347: 1–13.

Prince, R. C., and P. L. Dutton. 1978. Protonation and reduction potential of the primary electron acceptor. *In* The Photosynthetic Bacteria. R. K. Clayton and W. R. Sistrom, editors. Plenum Press, New York. 439–453.

Schenck, C. C., R. E. Blankenship, and W. W. Parson. 1982. Radical-pair decay kinetics, triplet yields and delayed fluorescence from bacterial reaction centers. *Biochim. Biophys. Acta.* 680:44–59.

Schowen, K. B. J., and R. L. Schowen. 1982. Solvent isotope effects on enzyme systems. *Methods Enzymol.* 87:551–606.

Sebban, P., P. Maróti, and D. K. Hanson. 1995. Electron and proton transfer to quinones in bacterial photosynthetic reaction centers: insight from combined approaches of molecular genetics and biophysics. *Biochimie.* 77:677–694.

Shinkarev, V. P., E. Takahashi, and C. A. Wraight. 1992. Electrostatic interactions and flash-induced proton uptake in reaction centers from *Rb. sphaeroides. In* The Photosynthetic Bacterial Reaction Center. II. Structure, Spectroscopy and Dynamics. J. Breton and A. Verméglio, editors. Plenum Press, New York. 375–387.

Shinkarev, V. P., M. I. Verkhovskii, and N. I. Zakharova. 1989. Influence of protonation of amino acid residues on electron transport in the complex of quinone acceptors of the reaction centers of the purple bacterium *Rhodobacter sphaeroides. Biokhimiya.* 54:256–264.

Shinkarev, V. P., and C. A. Wraight. 1993. Electron and proton transfer in the acceptor quinone complex of reaction centers of phototrophic bacteria. *In* The Photosynthetic Reaction Center, Vol I. J. Deisenhofer and J. R. Norris, editors. Academic Press, New York. 193–255.

Shinkarev, V. P., and C. A. Wraight. 1997. The interaction between quinone and detergent with reaction centers of purple bacteria. I. Slow quinone exchange between reaction center micelles and pure detergent micelles. *Biophys. J.* 72:2304–2319.

Stein, R. R., A. L. Castellvi, J. Bogacz, and C. A. Wraight. 1984. Herbicide-quinone competition in the acceptor complex of photosynthetic reaction centers from *Rhodopseudomonas sphaeroides*: a bacterial model for PS II-herbicide activity in plants. *J. Cell. Biochem.* 25: 243–259.

Stowell, M. H. B., T. M. Phillips, D. C. Rees, S. M. Soltis, E. Abresch, and G. Feher. 1997. Light-induced structural changes in photosynthetic reaction center: implications for mechanism of electron-proton transfer. *Science.* 276:812–816.

Takahashi, E., P. Maróti, and C. A. Wraight. 1992. Coupled proton and electron transfer pathways in the acceptor quinone complex of reaction centers from *Rhodobacter sphaeroides. In* Electron and Proton Transfer in Chemistry and Biology. A. Müller, H. Ratajczak, W. Junge, and E. Diemann, editors. Elsevier, Amsterdam. 219–236.

Takahashi, E., and C. A. Wraight. 1990. A crucial role for Asp^{L213} in the proton transfer pathway to the secondary quinone of reaction centers from *Rhodobacter sphaeroides. Biochim. Biophys. Acta.* 1020:107–111.

Takahashi, E., and C. A. Wraight. 1992. Proton and electron transfer in the acceptor quinone complex of *Rhodobacter sphaeroides* reaction centers: characterization of site-directed mutants of the two ionizable residues, Glu^{L212} and Asp^{L213}, in the Q_B binding site. *Biochemistry.* 31:855–866.

Verméglio, A. 1982. Electron transfer between primary and secondary electron acceptors in chromatophores and reaction centers of photosynthetic bacteria. *In* Function of Quinones in Energy Conserving Systems. B. L. Trumpower, editor. Academic Press, New York. 169–180.

Wraight, C. A. 1979. Electron acceptors of bacterial reaction centers. II. H^+ binding coupled to secondary electron transfer in the quinone acceptor complex. *Biochim. Biophys. Acta.* 548:309–327.

Wraight, C. A. 1981. Oxidation-reduction physical chemistry of the acceptor quinone complex in bacterial photosynthetic reaction centers: evidence for a new model of herbicide activity. *Isr. J. Chem.* 21: 348–354.

Wraight, C. A. 1982. The involvement of stable semiquinones in the two electron gates of plant and bacterial photosynthesis. *In* Function of Quinones in Energy Conserving Systems. B. L. Trumpower, editor. Academic Press, New York. 181–197.

Zhu, Z-Y., and S. Karlin. 1996. Clusters of charged residues in protein three-dimensional structures. *Proc. Natl. Acad. Sci. USA.* 93: 8350–8355.